Crystal structures of reduced and oxidized DsbA: investigation of domain motion and thiolate stabilization

Luke W Guddat[1], James CA Bardwell[2] and Jennifer L Martin[1]*

Background: The redox proteins that incorporate a thioredoxin fold have diverse properties and functions. The bacterial protein-folding factor DsbA is the most oxidizing of the thioredoxin family. DsbA catalyzes disulfide-bond formation during the folding of secreted proteins. The extremely oxidizing nature of DsbA has been proposed to result from either domain motion or stabilizing active-site interactions in the reduced form. In the domain motion model, hinge bending between the two domains of DsbA occurs as a result of redox-related conformational changes.

Results: We have determined the crystal structures of reduced and oxidized DsbA in the same crystal form and at the same pH (5.6). The crystal structure of a lower pH form of oxidized DsbA has also been determined (pH 5.0). These new crystal structures of DsbA, and the previously determined structure of oxidized DsbA at pH 6.5, provide the foundation for analysis of structural changes that occur upon reduction of the active-site disulfide bond.

Conclusions: The structures of reduced and oxidized DsbA reveal that hinge bending motions do occur between the two domains. These motions are independent of redox state, however, and therefore do not contribute to the energetic differences between the two redox states. Instead, the observed domain motion is proposed to be a consequence of substrate binding. Furthermore, DsbA's highly oxidizing nature is a result of hydrogen bond, electrostatic and helix-dipole interactions that favour the thiolate over the disulfide at the active site.

Addresses: [1]Centre for Drug Design and Development, University of Queensland, Brisbane, QLD, 4072, Australia. [2]Department of Biology, University of Michigan, Ann Arbor, MI, 48109-1048, USA.

*Corresponding author.
E-mail: j.martin@mailbox.uq.edu.au

Key words: disulfide bond, DsbA, protein folding, protein structure, thioredoxin fold

Received: **16 March 1998**
Revisions requested: **14 April 1998**
Revisions received: **20 April 1998**
Accepted: **20 April 1998**

Structure 15 June 1998, **6**:757–767
http://biomednet.com/elecref/0969212600600757

Introduction

DsbA is one of a family of disulfide oxidoreductase proteins that share a common domain structure, the thioredoxin fold [1]. In addition to the bacterial disulfide catalyst DsbA, the thioredoxin-fold family includes the eukaryotic protein disulfide isomerase (PDI) and the ubiquitous reductants, thioredoxin and glutaredoxin. Numerous other proteins of varying sequence length that catalyze a range of disulfide exchange reactions [2–5] incorporate the classic thioredoxin active-site motif Cys–X–X–Cys (and presumably the thioredoxin fold) in divergent but recognizably homologous sequences.

Within the subset of thioredoxin fold proteins that catalyze disulfide-exchange reactions, and for which three-dimensional structures are known, the thioredoxin domain is utilised in a variety of ways to perform a wide range of redox reactions. Thus, thioredoxin and glutaredoxin include only the thioredoxin domain in their three-dimensional structure — they are single-domain monomeric proteins. DsbA is also a monomer, but is twice the size of glutaredoxin and thioredoxin. The structure of DsbA incorporates both a thioredoxin domain and a helical domain, which is inserted into the thioredoxin domain (Figure 1; [6]). Finally, PDI is dimeric with each 57 kDa monomer organised into four thioredoxin domains [7]. The first two proteins, glutaredoxin and thioredoxin, are both reducing, but thioredoxin is a more general protein reductant than glutaredoxin [8]. In contrast, DsbA and PDI are both oxidizing proteins. Both have broad substrate specificity; DsbA functions almost exclusively as an oxidant, PDI can also catalyze disulfide rearrangement [9].

The common thioredoxin folds in each of these four proteins are very similar [1,7,10], incorporating a four-stranded β sheet and three helices. One of the two active-site cysteines, the more N-terminal of the two in sequence, protrudes from the surface of the thioredoxin-like proteins. In all these proteins this cysteine is the reactive cysteine that interacts with the substrate cysteine.

Despite the high degree of structural similarity, the thioredoxin-like proteins vary widely in their oxidizing power. Because the redox power of these proteins closely reflects their function, an important goal in analyzing the function of these proteins is the elucidation of how such a wide variation in redox potential is produced within equivalent structural frameworks.

Figure 1

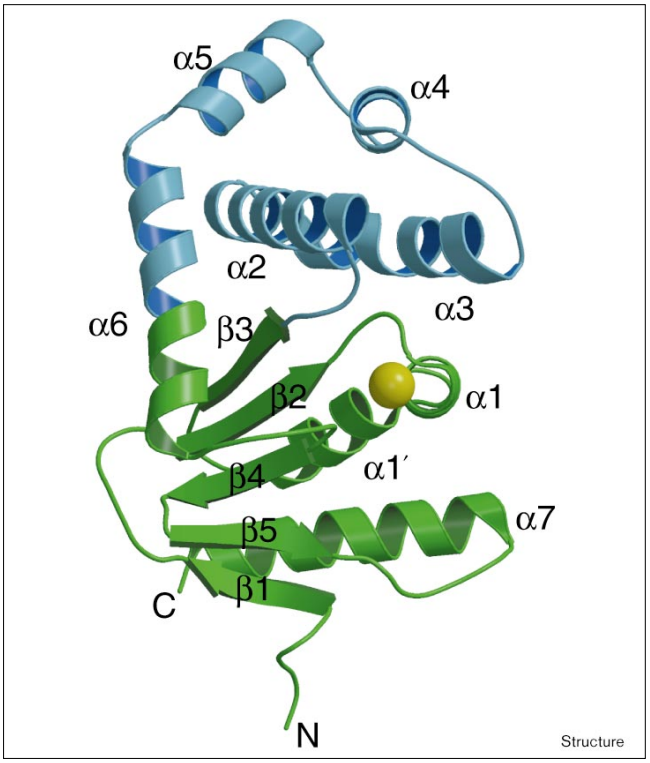

A schematic representation of DsbA with helices shown as coils and strands as arrows. The thioredoxin domain is in green and the helical domain is in blue. The N and C termini are labeled and the active-site Cys30 sulfur atom is shown as a yellow CPK sphere. The putative peptide-binding groove is bounded by the active-site helix α1/α1′ and the flexible loop between β5 and α7. This figure was generated using MOLSCRIPT v2.0.1 [52] and Raster3D [53,54].

DsbA functions as a protein oxidant in the bacterial periplasm and is by far the most oxidizing of the thioredoxin-like proteins, with a redox equilibrium constant for the reaction with glutathione of 0.1 mM [11,12]. In comparison, the value for PDI is ~1 mM [13,14] and for the reducing protein thioredoxin it is 10 M [15]. Thus, DsbA strongly favours formation of oxidized glutathione, whereas the reverse is true for thioredoxin. The extreme nature of DsbA's redox potential should simplify the recognition of redox determinants of this protein in comparison to thioredoxin, the most reducing of these proteins.

We are assisted in our work by a large amount of biochemical, structural and genetic information on DsbA. DsbA has two unusual properties that are thought to contribute to its highly oxidizing nature. First, although disulfides generally stabilize proteins, oxidized DsbA is less stable than reduced DsbA [12,16]. Second, the pK_a of the accessible cysteine (Cys30) in the active site of DsbA is strongly perturbed from the normal value of ~9 to a very low value of 3.5 [17,18]. This implies that at physiological pH, Cys30 is fully ionized to the thiolate form.

The unusual stability of reduced DsbA, and hence its strongly oxidizing nature, may be explained either by electrostatics at the active site or by domain motion — or a combination of both. In the electrostatic model, the reduced form of DsbA is energetically preferred through stabilization of the Cys30 thiolate [17,19]. In the domain motion model, the energy difference between oxidized and reduced DsbA is a result of redox-dependent conformational changes [20,21] and provides the thermodynamic drive favoring transfer of disulfide from DsbA to substrate. We have previously proposed the possibility of hinge bending motion in DsbA and have identified a β turn connecting the two domains as a possible hinge point for domain motion [20].

The question of why DsbA is so oxidizing is addressed here at the molecular level by a structural comparison of oxidized DsbA with reduced DsbA. We present an analysis of two independent structures of reduced DsbA and five independent structures of oxidized DsbA. A comparison of these structures reveals that local conformational changes occur at the active site in response to active-site disulfide reduction, resulting in a network of stabilizing interactions around the active-site thiolate. Domain motion is not correlated with this redox state change, but may be associated with substrate binding near the active site.

Results

Redox structures of DsbA

To elucidate the reasons for DsbA's extremely oxidizing redox potential we have determined the crystal structure of reduced DsbA and compared it with structures of oxidized DsbA. We have two independent structures of reduced DsbA (non-crystallographic symmetry-related structures), and five independent structures of oxidized DsbA, three of which are from two new crystal forms. These crystal structures, derived from varying crystallization conditions (pH range 5–6.5) and with very different crystal lattice contacts, provide an ideal platform for understanding how the redox state affects the conformation and function of DsbA.

The previously reported crystal structure of oxidized DsbA (OX1; [6,20]) was determined at pH 6.5 from a monoclinic crystal form, with two molecules in the asymmetric unit (OX1A and OX1B). The three newly determined crystal structures are: reduced DsbA (RED) at pH 5.6 in an orthorhombic crystal form, including two copies of the protein in the asymmetric unit (REDA and REDB); oxidized DsbA (OXR), which was produced from a crystal of reduced DsbA that was oxidized by withholding addition of reducing agent after crystal formation (this oxidized DsbA structure is in the same crystal form and at the same pH as the reduced DsbA structure and also has two independent copies in the asymmetric unit, OXRA and OXRB); and oxidized DsbA (OX2) at pH 5.0 in a monoclinic crystal form, with one molecule in the asymmetric unit.

Crystallographic and geometric statistics for the three new crystal structures are given in Tables 1 and 2. Figure 2 shows the electron density in the active-site region of reduced and oxidized DsbA from the orthorhombic crystal form.

A comparison of DsbA redox structures

The structural similarity of each of the DsbA structures described above was analyzed pairwise by measuring the root mean square deviation (rmsd) for Cα atoms of all residues (Table 3, normal text). Most pairs of structures were very similar, having rmsd values for all Cα atoms of 0.5–0.6 Å. The largest difference between any pair of structures is 0.92 Å. This difference is for the comparison of a reduced and oxidized pair of structures determined at the same pH (REDA and OXRB). In contrast, a comparison of the two reduced DsbA structures in the same crystal form and at the same pH (REDA and REDB) gives an rmsd of 0.55 Å. This result on its own could be taken to indicate that a significant conformational change occurs upon oxidation of the active-site cysteines. Other lines of evidence do not support this, however. First, the other three pairs of reduced and oxidized structures at the same pH have much lower rmsd values (< 0.57 Å). Second, three of the four pairs of DsbA structures with the lowest rmsd (< 0.5 Å) are for comparisons of oxidized and reduced DsbA structures over a wide range of pH values. Finally, two of the four pairs of DsbA structures having the largest rmsd values (> 0.90 Å) are for comparisons of oxidized DsbAs. Overall, these results show that there is no large structural change upon reduction of the active-site disulfide of DsbA.

Table 1

Crystallographic data.

	RED	OXR	OX2
Unit cell			
a	88.9	89.4	38.5
b	83.4	83.8	51.4
c	58.3	58.9	42.5
α	90.0	90.0	90.0
β	90.0	90.0	103.1
γ	90.0	90.0	90.0
Space group	$P2_12_12$	$P2_12_12$	$P2_1$
Solvent (%)	49	49	37
Molecules in asymmetric unit	2	2	1
Resolution range	50–2.7	50–2.7	50–2.0
Observations (I > 1σ(I))	18,501	43,081	38,303
Unique reflections (I > 1σ(I))	9,160	10,864	10,434
Outer shell	2.8–2.7	2.8–2.7	
2.07–2.0			
Rsym* (%)	11.8	8.3	4.6
Rsym* (outer shell) (%)	29.4	29.8	15.3
I/σ(I)	7.0	13.0	16.0
I/σ(I) (outer shell)	2.2	3.2	7.4
Completeness (%)	73.6	86.1	94.2
Completeness (outer shell; %)	56.1	69.9	81.6

*Rsym = $\Sigma|I - \langle I\rangle|/\Sigma\langle I\rangle$.

We also determined how similar the isolated thioredoxin domains in the different crystal forms were to each other and how similar the helical domains were to each other (Table 3, bold text). The results from this individual domain comparison suggest that the domains are very similar between the different crystal structures and that there is no correlation between a lower rmsd and the same redox state. For example, the thioredoxin domains of a reduced and oxidized pair of structures (REDA and OX2) are the most similar of any pair (rmsd 0.32 Å).

The pairs of structures with the largest rmsd values in the overall comparison had significantly lower rmsd values for the single domain comparisons (see for example REDA and OX1A). Further analysis of all the structures revealed that the domains of DsbA can move relative to one another, in a hinge bending motion (Figure 3).

Domain motion does not correlate with redox state

Previously, we have hypothesised that the two domains of DsbA can move relative to one another and that this could be a means of stabilizing the reduced relative to oxidized DsbA [20,21]. A putative hinge region was identified: a loop of residues (Phe63–Met64–Gly65–Gly66) forming a type IV β turn connecting the thioredoxin and helical domains. The other connection between the two domains of DsbA is helix α6. This helix corresponds to helix α3 in thioredoxin, but is extended by two turns in DsbA and can be considered to be part of either domain in DsbA (Figure 1). Using the program HINGEFIND [22], we analyzed the hinge bending that occurs between the two domains for each pair of structures. We found that the hinge bending angle between the helical domain and the thioredoxin domain varies by as much as 7° among the seven DsbA structures. The three pairs of non-crystallographic symmetry-related DsbA structures (OX1A and OX1B, OXRA and OXRB, REDA and

Table 2

Crystallographic refinement statistics.

	RED	OXR	OX2
Resolution range (Å)	50–2.7	50–2.7	50–2.0
Number of reflections (F > 1σF)	8,931	10,710	10,332
R-factor*	0.233	0.261	0.182
R-free†	0.285	0.308	0.227
Number of waters	16	25	90
Average B-factor (Å^2)	31.2	24.2	23.6
Rmsd from ideal			
Bond length (Å)	0.004	0.004	0.005
Bond angle (°)	0.89	0.94	1.00
Dihedral angle (°)	22.2	23.2	22.4
Improper angle (°)	0.87	0.89	0.96
Ramachandran statistics			
Residues in most favoured region (%)	89.0	88.3	93.4
Residues in disallowed regions (%)	0	0	0

*R-factor = $\Sigma \mid F_o - F_c \mid / \Sigma F_o$. †R-free as defined by Brünger [48].

Figure 2

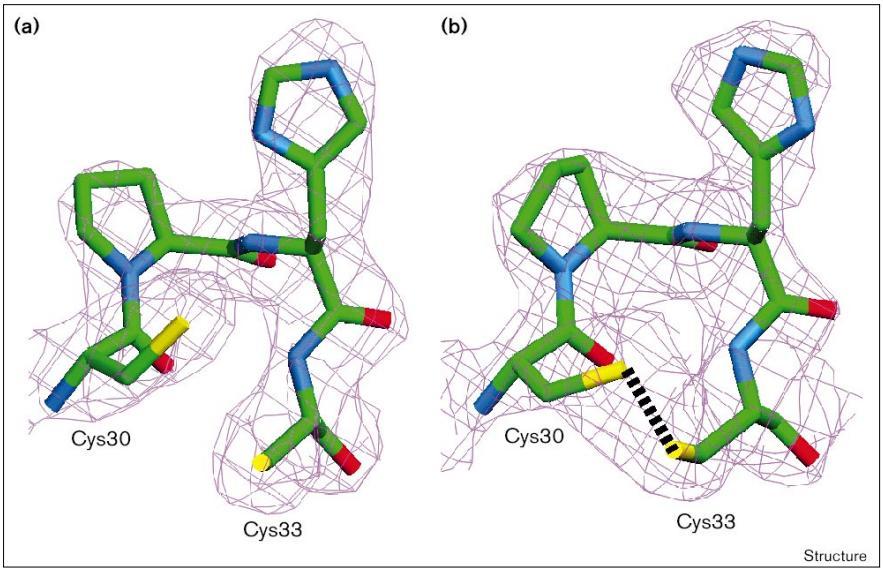

An electron density map ($2F_o–F_c$, 1σ) for residues Cys30–Pro31–His32–Cys33 at the active site of DsbA showing **(a)** the reduced thiols in REDB and **(b)** the disulfide bond in OXRB. This figure was generated using Setor v5.0 [55].

REDB), for which one might expect the smallest domain-angle differences, have hinge bend angles of 3.5–4°. The largest values (6–7°) represent a closure of the helical domain of REDA or OX2 when compared with OX1A, OX1B or OXRB. In contrast, one of the smallest hinge bend angles (1.5°) occurs for the comparison of REDA and OX2 — structures of different redox forms, crystallized at different pH and in different crystal lattices. These results confirm that there is no correlation between redox state and domain movement in these crystal structures.

Domain closure may occur upon peptide–groove interaction

If the domain motion in DsbA is not redox related, what causes the hinge bending in these different structures?

Table 3

A comparison of oxidized and reduced DsbA.

	OX1A	OX1B	OX2	OXRA	OXRB	REDA	REDB
OX1A		**0.35**	**0.59**	**0.50**	**0.39**	**0.54**	**0.35**
		0.38	**0.35**	**0.40**	**0.35**	**0.40**	**0.32**
OX1B	0.57		**0.45**	**0.40**	**0.39**	**0.41**	**0.35**
			0.36	**0.39**	**0.46**	**0.38**	**0.34**
OX2	0.91	0.69		**0.45**	**0.58**	**0.32**	**0.43**
				0.42	**0.38**	**0.27**	**0.25**
OXRA	0.63	0.56	0.62		**0.47**	**0.42**	**0.43**
					0.45	**0.39**	**0.41**
OXRB	0.46	0.59	0.91	0.62		**0.52**	**0.38**
						0.45	**0.41**
REDA	0.90	0.73	0.38	0.57	0.92		**0.39**
							0.30
REDB	0.55	0.48	0.54	0.45	0.56	0.55	

Normal text, rmsd (Å) for 186 Cα atoms (residues 3–188); bold text, rmsd (Å) for 95 Cα atoms in the thioredoxin domain (residues 7–14, 19–63, 139–166, 173–186) and 75 Cα atoms in the helical domain residues (64–138).

The reason appears to be crystal contacts that specifically involve the putative peptide-binding groove (bound by the active-site helix α1/α1′ and the loop connecting strand β5 and helix α7). In OX2, these interactions are formed between the crystallographic symmetry-related residues Ser128*–Phe129*–Val130* and residues of the groove (Figure 4). Phe129* binds deep within the peptide groove and forms hydrophobic interactions with residues Pro163, Phe174 and the sidechain carbons of Gln164 and Thr168. In addition, symmetry-related Val130* forms hydrophobic interactions with Met171 and Thr168.

Similarly, in REDA the symmetry-related residues Val196A*–Gln97A*–Lys98A*–Thr99A*–Gln100A* interact with the peptide-binding region and in REDB there are interactions with Arg103A*, Ser104A*, Asp172B* and Val173B*. In both reduced structures, however, the symmetry-related residue interactions with the peptide groove are not as deep as those observed in OX2. Curiously, the two oxidized DsbA structures OXRA and OXRB, derived from crystals of reduced DsbA that were allowed to oxidize, have somewhat different crystal contacts to the equivalent REDA and REDB structures (cell edges increase by ~0.5 Å in OXR compared with RED, Table 1). The altered crystal contacts result in small differences (~3°) in the hinge bend angle for OXRA/REDA and OXRB/REDB. These differences result from a re-packing of the symmetry-related molecules in OXR compared with RED to accommodate local structural changes at the active site (see below).

The structural consequence of interactions between symmetry-related residues and the peptide groove in DsbA is a widening of the groove, resulting from an increased separation of the flexible loop and the active-site helix. The

Figure 3

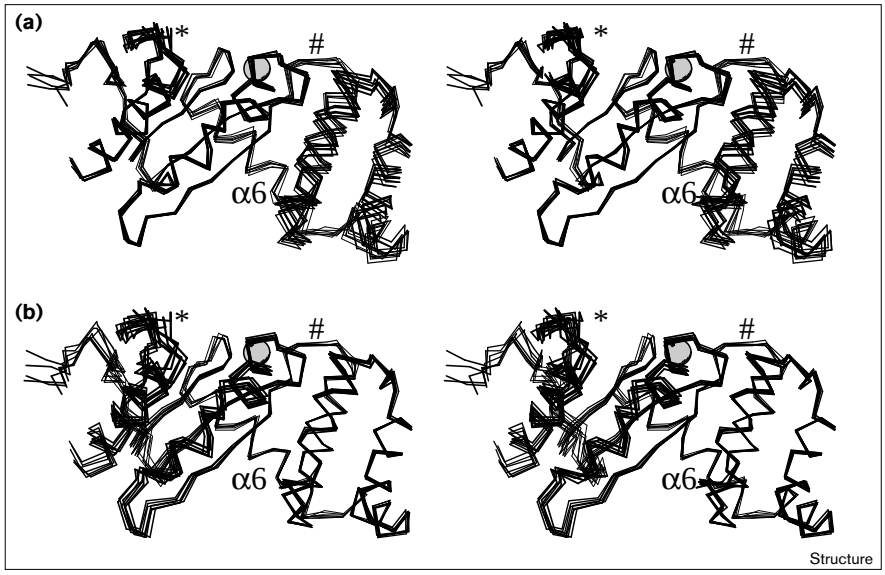

A stereo view of the superimposition of backbone Cα traces of the five oxidized and two reduced DsbA crystal structures. **(a)** The superimposition using residues from the thioredoxin domain (7–14, 19–63, 139–166 and 173–186) and **(b)** the superimposition using residues from the helical domain (64–138). The active-site Cys30 sulfur atom is shown as a CPK sphere. The flexible loop, indicated by an asterisk, forms one edge of the putative peptide-binding groove. The two domain connections (the β-turn, indicated by a hash sign, and helix α6) are also indicated. This figure was generated using MOLSCRIPT v2.0.1 [52].

movement of the active-site helix transmits to the helical domain and the overall effect is a small but significant hinge bending closure of the helical domain with respect to the thioredoxin domain. This hinge closing movement may be biologically relevant because the interactions observed in the crystal could be representative of the interactions that occur between substrate and DsbA. Thus, an interaction between unfolded polypeptide substrate and DsbA could well involve hydrophobic interactions like those observed in the symmetry-related contacts and could therefore result in domain closure.

Thiolate stabilization in reduced DsbA

As described above, no large conformational change occurs upon disulfide reduction in the crystal structures of DsbA described here. Where differences in domain orientation are observed, these correlate with crystal contacts involving peptide–groove interactions, rather than with the redox state of the protein. What then are the differences between the oxidized and reduced structures of DsbA that could account for the stability difference between the two redox states?

The very low pK_a of Cys30 means that this thiol group is ionized (thiolate) when DsbA is in the reduced form. The crystal structure of reduced DsbA, determined at pH 5.6, provides us with two independent views — REDA and REDB — of this Cys30 thiolate redox form. In comparison with the oxidized DsbA structures, the sidechain of Cys30 in both REDA and REDB moves to a much greater extent (up to a 1 Å shift of Cys30 Sγ) than that of Cys33 (Figure 5). In addition, the surface accessibility of Cys30 Sγ increases by 5–10% whereas Cys33 Sγ is completely buried in both redox states.

Figure 4

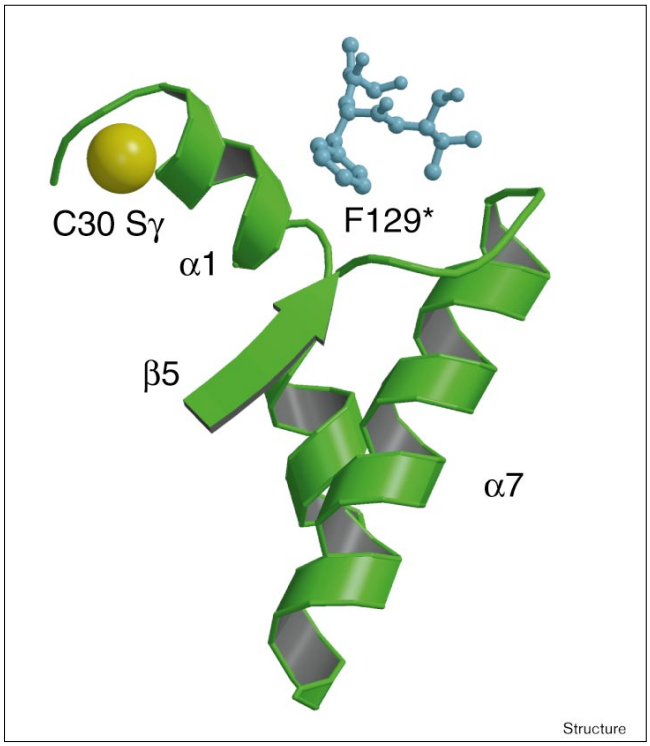

Symmetry-related contact in the OX2 crystal structure at the proposed peptide-binding groove of DsbA. The groove is formed between the active-site helix (α1) on the left and the β5 strand–loop–α7 helix on the right. The symmetry-related atoms Ser128*–Phe129*–Val130* are shown in a blue ball-and-stick representation, with Phe129* labeled (F129*). The active-site Cys30 sulfur atom is shown as a yellow CPK sphere. This figure was generated using MOLSCRIPT v2.0.1 [52] and Raster3D [53,54].

Figure 5

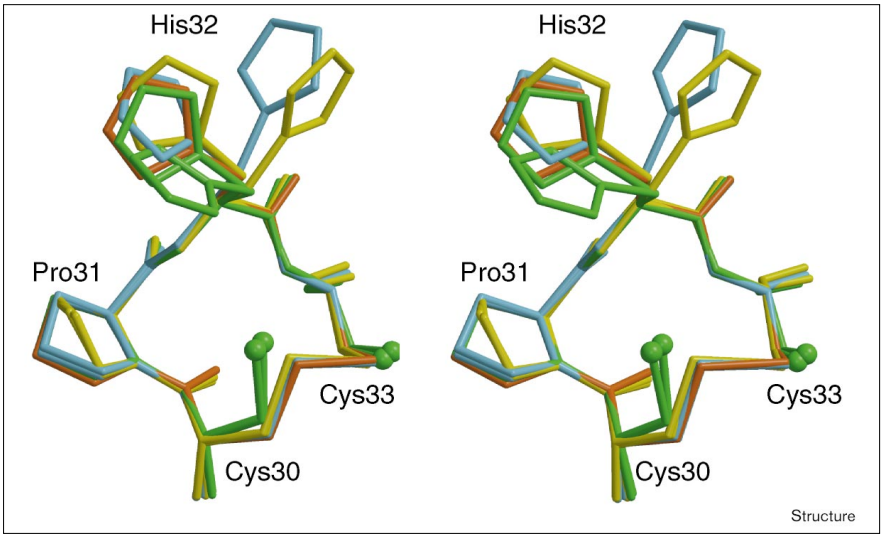

A stereo view of the superimposition of the active-site residues Cys30–Pro31–His32–Cys33 for the five oxidized and two reduced DsbA structures. The reduced DsbA structures (REDA, REDB) are shown in green (His32 of REDA is closer to the Cys30 sidechain than that of REDB) and the equivalent oxidized DsbA structures (OXRA, OXRB) are shown in yellow (His32 of OXRA is farthest from the Cys30 sidechain). The two OX1 structures are in light blue and the low pH oxidized structure (OX2) is in orange. This figure was generated using MOLSCRIPT v2.0.1 [52] and Raster3D [532,54].

In both REDA and REDB, the Cys30 thiolate is stabilized by several interactions (Table 4, Figure 6). One of these is a hydrogen bond formed between the Cys30 Sγ thiolate and the thiol of Cys33. Two other hydrogen bonds further stabilize the Cys30 Sγ thiolate; these are interactions with the backbone amide nitrogens of His32 and Cys33. In the oxidized structures of DsbA, the hydrogen bond between Cys30 Sγ and the Cys33 amide is present, but the interaction with the His32 amide is absent.

Mutagenesis studies show that His32 is important for the redox stability profile of DsbA [18]. It has been suggested that the Cys30 Sγ thiolate is stabilized by a favourable electrostatic interaction with the sidechain of His32. The structures of reduced DsbA described here lend support to this hypothesis because they indicate a movement of His32 towards the Cys30 sidechain, compared with the oxidized structures (Figure 5). In the case of REDA, the Cys30 Sγ and His32 Nδ1 atoms are within hydrogen-bonding distance (3.6 Å, Figure 6). For REDB this distance is 4.5 Å, but is nonetheless 1–2.5 Å shorter than the oxidized DsbA crystal structures. Strangely, the most dramatic difference in the His32 conformation in all these crystal structures is for the comparison of REDA and OXRA — the reduced and oxidized forms of DsbA from the same crystal form. For these two structures, the His32 χ1 sidechain dihedral differs by 120° (Figure 5). This difference gives rise to different crystal packing in this

Table 4

Interatomic distances* at the active site.

	OX1A	OX1B	OX2	OXRA	OXRB	REDA	REDB
30Sγ–33Sγ	2.0	2.0	2.0	2.0	2.0	3.5	3.4
30Sγ–32N	4.0	4.1	4.0	3.8	3.8	3.6	3.4
30Sγ–33N	3.1	3.2	3.2	3.0	3.1	3.6	3.3
30Sγ–32Nδ1	5.8	7.0	6.8	5.6	6.6	3.6	4.5
33Sγ–27N	3.9	4.0	3.8	3.9	3.7	3.7	3.8
33Sγ–27O	3.9	4.1	3.9	3.9	3.8	4.0	4.0
33Sγ–30O	4.0	4.1	3.9	3.8	3.9	4.3	4.5

*Distances are given in Å. The hydrogen bond distance between two thiol groups is usually 3.8 Å; between thiol and nitrogen or oxygen atoms, the hydrogen bond distance is usually 3.3–3.6 Å [29–31].

Figure 6

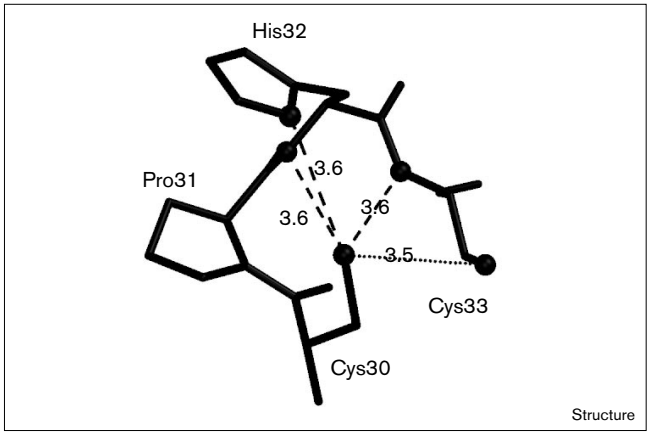

The active-site residues of REDA, shown in the same orientation as that used in Figure 5. The atoms Cys30 Sγ, His32 N and Nδ1, Cys33 N and Sγ are shown as spheres. Hydrogen bond interactions with Cys30 thiolate are shown as dashed lines. The interaction between Cys30 thiolate and Cys33 thiol is shown as a dotted line. Distances for these interactions are shown in Å. This figure was generated using MOLSCRIPT v2.0.1 [52].

region and results in a different domain hinge angle, as described above.

A comparison with thioredoxin

To investigate why the active-site disulfide is destabilizing in DsbA but stabilizing in structurally related proteins, we also compared the structures of the very oxidizing DsbA with oxidized and reduced structures of the most reducing member of the family, thioredoxin. Three groups have determined structures for the two redox forms of thioredoxin. The NMR solution structures of reduced and oxidized *Escherichia coli* [23] and human [24] thioredoxin are available. Furthermore, crystal structures of the two redox forms of human thioredoxin are also published [25]. Coordinates for all these structures are available from the Protein Data Bank [26].

As we observed for DsbA, there are no large conformational differences between the reduced and oxidized structures of thioredoxin. The structural differences that are observed, are small and localized to the active site. Thus, upon active-site reduction, the NMR structures of *E. coli* thioredoxin and the crystal structures of human thioredoxin show a larger change in position of the more N-terminal cysteine in the active site compared with the C-terminal cysteine. In the NMR structure of human thioredoxin, however, a larger change is observed for the more C-terminal cysteine.

In the crystal structure of reduced DsbA, we observe a hydrogen bond between the sidechain sulfurs of the two active-site cysteines. Similarly, in the NMR structure of *E. coli* thioredoxin and the crystal structure of human thioredoxin, a hydrogen bond of 3.8–3.9 Å is observed between the sidechain of the Cys30 equivalent and the thiol of the Cys33 equivalent [23,25]. In the NMR structure of human thioredoxin, however, the average distance for this bond is a very short 3.1 Å [24]. This may be the result of a soft non-bonded potential used in the structure refinement [23].

The crystal structures of both reduced and oxidized DsbA reveal a hydrogen bond between Cys30 and the amide nitrogen of Cys33. Curiously, the interaction with the Cys33 equivalent mainchain amide is observed only in the oxidized forms of the NMR structure of *E. coli* and the crystal structure of human thioredoxin, and is absent in the corresponding reduced structures. This hydrogen bond is observed in both oxidized and reduced forms of the NMR structures of human thioredoxin, however.

Reduced DsbA is also stabilized by a hydrogen bond between the Cys30 thiolate and the mainchain amide of His32. In addition, an electrostatic interaction is found in the crystal structure of reduced DsbA between His32 and Cys30, which can further stabilize the reduced form. In thioredoxin, the residue equivalent to His32 is a highly conserved proline. Unlike other residues, proline cannot donate a mainchain hydrogen bond and, unlike histidine, it cannot provide sidechain stabilization of the thiolate by either electrostatic or hydrogen bond interactions. The structure of reduced mutant T4 glutaredoxin [27], which, like thioredoxin, also has the active-site sequence Cys–Gly–Pro–Cys, has similar interactions at the active site as those described for thioredoxin.

Discussion

The extremely oxidizing nature of DsbA has been proposed to result from a conformational change of the two domains upon active-site disulfide reduction (to relieve strain in the oxidized form) or from the stabilization of the active-site Cys30 thiolate in the reduced form. The DsbA structures presented here show that hinge bending motion of the two domains is permitted. This hinge motion is not correlated with redox state, however, but is a result of interactions at the putative peptide-binding groove of DsbA. These results therefore suggest that domain motion is not a valid model to explain the oxidizing properties of DsbA. The hinge bending motion of DsbA could, however, be significant for substrate binding and/or for interactions with other proteins such as DsbB [28].

In favour of the thiolate stabilization hypothesis, the crystal structure of reduced DsbA reveals an intricate network of favourable interactions with Cys30 thiolate that are not present in oxidized DsbA. First, a hydrogen bond is formed between the Cys30 thiolate and the sidechain thiol of Cys33. The interatomic distance between the two sulfur atoms in DsbA is relatively short (3.4–3.5 Å) compared with the 3.8 Å hydrogen bonds observed in the neutron diffraction study of L-cysteine [29] and in NMR [23] and crystal structures [25] of reduced thioredoxin. This shorter interaction could be an important component of both the increased stabilization of reduced compared with oxidized DsbA, as well as in the comparison of DsbA with related redox proteins such as thioredoxin. The difference between the sulfur–sulfur distance in reduced DsbA and thioredoxin may not be significant, however, given the resolution of the reduced DsbA structure (2.7 Å) and the use of different refinement parameters.

Other interactions that stabilize the Cys30 thiolate of reduced DsbA include two hydrogen bonds with mainchain amides of His32 and Cys33. These interactions are within the usual limits (3.3–3.6 Å) for S–N hydrogen bonds [29–31]. The second of these hydrogen bonds is also present in the oxidized structure of DsbA. However, hydrogen bonds involving charged groups (such as the thiolate in the reduced form) are more energetically favourable [32,33] than those involving uncharged groups (such as the half-cysteine of the disulfide bond). Thus, even though the hydrogen bond with the Cys33 backbone amide may be

present in both the oxidized and the reduced DsbA structures, it is likely to stabilize the reduced form more than it stabilizes the oxidized form. The first of these two hydrogen bonds is not possible in thioredoxin, in which the highly conserved histidine residue of DsbA is replaced with the highly conserved proline of thioredoxin. Furthermore, the interaction between the reactive thiolate and the mainchain amide of the Cys33 backbone amide is observed in only one of three independently determined reduced thioredoxin structures.

The histidine between the two cysteines is critical for the stability profile of DsbA [18]. A histidine at the N terminus of a helix, such as His32 in DsbA, is unfavourable because of the interaction with the helix dipole [34]. His32, however, forms at least two stabilizing interactions with the thiolate in reduced DsbA, through the amide backbone hydrogen bond and the sidechain electrostatic interaction. Thus, His32 destabilizes the oxidized form far more than it does the reduced form of DsbA. In comparison, the proline at this position in thioredoxin does not interact unfavourably with the helix dipole and cannot form the stabilizing backbone hydrogen bond or sidechain electrostatic interaction with the thiolate in the reduced form. So, these interactions that significantly effect the stability profile of DsbA are absent in the reducing protein thioredoxin.

Finally, the interaction between the active-site thiolate and the partial positive charge of the helix dipole also favours reduced over oxidized DsbA. This interaction is possible for all thioredoxin-like redox proteins, however, because a cysteine at the beginning of a helix forms part of the conserved active-site sequence. Indeed, a cysteine at the N terminus of any helix is highly favoured as a result of the interaction with the helix dipole [35] and leads to a reduction in the cysteine pK_a compared with the normal value (~9). All four of the thioredoxin family of redox proteins exhibit a reduced pK_a for this cysteine, although the pK_a of ~6–7 for thioredoxin [36–38] is somewhat higher than the pK_a values of 3.5–4.5 measured for DsbA [17,18], glutaredoxin [39–41] and PDI [19].

For the thioredoxin-fold redox proteins, the common stabilizing interactions for cysteine thiolate are therefore the interaction with the helix dipole and the hydrogen bond formation with the other active-site cysteine. These may be the only stabilizing interactions for thioredoxin. For DsbA, PDI and glutaredoxin there must be additional stabilizing interactions to account for the lower cysteine pK_a. For DsbA, the additional stability could derive from a combination of the shorter hydrogen bond formed with Cys33, the two additional hydrogen bonds formed with mainchain amides in the active site and the electrostatic interaction with His32. These same factors could also account for the lowered pK_a of PDI, which has a histidine at the equivalent position to DsbA.

Recently, we learned that an NMR solution structure of reduced DsbA has been determined that shows a larger hinge motion than described here [42]. This may be a result of the differing conditions under which the structures were determined. The reduced NMR structure was determined at pH 3.7 (a pH at which many acidic groups including Cys30 are most likely to be partially charged), whereas the crystal structure was determined at the somewhat more physiological pH of 5.6 (at which Cys30 is most likely to be fully ionized). The NMR structure determination of oxidized DsbA at pH 3.7 is underway (HJ Schirra, R Glockshuber *et al.*, personal communication) and will allow a better understanding of the difference between the NMR and crystal structures of reduced DsbA.

Biological implications

Divergent protein function within a similar protein fold is a repeating theme in biology. A detailed knowledge of how the function of structurally related proteins is controlled has broad implications for other systems. Within the family of thioredoxin fold proteins there exists a wide diversity of properties and functions, generally involving cysteine chemistry. Of the redox proteins in this family —including thioredoxin and DsbA —the redox strengths vary by a factor of 100,000. The most oxidizing of these proteins, the bacterial protein-folding factor DsbA, is unusual in that the redox state in which the two active-site cysteines are reduced is significantly more stable than the oxidized (or disulfide) form. Nevertheless, the thioredoxin folds of the highly oxidizing DsbA and the highly reducing thioredoxin are structurally equivalent.

Analysis of the structures of these two proteins can provide information about the factors that might affect function. A significant structural difference is the presence of two domains in DsbA, but only a single domain in thioredoxin. The possibility that domain flexibility in DsbA might account for its extremely oxidizing nature was investigated. We observed that hinge bending does occur between the two domains of DsbA. This conformational change was not correlated with redox state, however, and so does not contribute to the oxidizing nature of DsbA. Instead, domain motion may be required to facilitate protein–protein interactions such as those that occur with unfolded polypeptide substrate and/or with the re-oxidizing protein DsbB [28].

The greater stability of reduced over oxidized DsbA appears to be a result of a greater stabilization of the reactive thiolate (compared with the disulfide form) at the active site. This is affected by a network of hydrogen bond and electrostatic interactions that favour the formation of the Cys30 thiolate. These interactions include hydrogen bonds between the thiolate and the Cys33 thiol, the backbone nitrogen of Cys33 and the backbone

nitrogen of His32. The Cys30 thiolate can also form a favourable electrostatic/hydrogen bond interaction with the sidechain of His32. In addition, the thiolate of reduced DsbA can interact favourably with the helix dipole. These favourable interactions are removed in oxidized DsbA when Cys30 forms one half of the active-site disulfide. In contrast, the unfavourable interaction between His32 and the helix dipole is present in both the oxidized and reduced forms of DsbA.

Materials and methods

Expression, purification and crystallization

Recombinant DsbA was expressed and purified in *E. coli* as described previously [43]. Samples for crystallization were purified by FPLC using an HR 5/5 Mono Q column and concentrated to 40–60 mg/ml. Purity was estimated to be > 95% as judged by FPLC, SDS-PAGE and mass spectrometry.

Reduced DsbA (RED) was crystallized by the dialysis method; 3 µl each of protein (60 mg/ml) and precipitant were dispensed into 5 µl dialysis buttons (obtained from Hampton Research, California). We found that using a total volume of 6 µl rather than 5 µl helped prevent air bubbles forming when the dialysis buttons were sealed. Spectra/Por CE dialysis membrane, with a 15,000 Da molecular weight cut off, was used to seal the dialysis buttons. After sealing, the dialysis button was placed in a well of a Linbro tissue culture plate and immersed in 1.5 ml of precipitant solution. The precipitant solution consisted of 0.2 M ammonium acetate, 0.1 M sodium citrate pH 5.6, 30% w/v polyethylene glycol 4 K and 40 mM dithiothreitol (DTT). The wells were then sealed with cover slips and white soft paraffin. Reduced DsbA crystals of average size $0.3 \times 0.1 \times 0.1$ mm^3 appeared within 2–3 days. Additional DTT (10 µl of a 1 M stock solution) was added to the precipitant solution every 2–3 days to ensure DsbA was maintained in the reduced form. Isoelectric focusing gels of samples taken from the equilibrated protein in the dialysis button confirmed that DsbA was in the reduced form.

Crystallization and structure determination of the original crystal form of oxidized DsbA (OX1) has been described in detail previously [44]. Briefly, the crystals are grown by hanging drop vapour diffusion using a precipitant of 25% polyethylene glycol 8 K in 0.1 M cacodylate buffer, pH 6.5. Two new crystal forms of oxidized DsbA were prepared for this work. One (OXR) was produced by dialysis in the same way as reduced DsbA crystals, but was oxidized over a period of two months by withholding addition of DTT after crystallization. The other oxidized DsbA crystal form (OX2) was grown using the hanging drop vapour diffusion method. Drops of 4 µl were used (2 µl each of 40 mg/ml DsbA and reservoir). The reservoir consisted of 27% polyethylene glycol 4 K in 0.1 M acetate buffer, pH 5.0. Crystals grew within 1–2 weeks and were of average size $0.5 \times 0.4 \times 0.2$ mm^3.

Crystallographic data measurement

Unit cell, space group and crystallographic statistics for data from each of the three new crystal forms of DsbA are presented in Table 1. For OX2, OXR and RED, data were measured at 16°C using a RAXIS-IIC image plate area detector with RU-200 rotating anode X-ray generator operated at 46 kV and 60 mA. The crystal to detector distance was 100 mm and each frame was exposed for 30 min with an oscillation range of 2°. Frames were integrated, scaled and merged using the DENZO and SCALEPACK programs [45].

Reduced DsbA crystals are radiation sensitive, resulting in a reduction of diffraction data quality over time. We have not been able to overcome this problem using cryogenic data measurement because suitable cryoprotectant solution conditions and soaking regimes (which do not crack crystals, or increase mosaicity to > 1°) have not been identified.

Structure determination

The structure of OX1 (PDB accession code 1FVK) was used as the search model to solve the structures of OX2 and RED by molecular replacement [46] using X-PLOR v3.1 [47] and v3.851, respectively. The structure of OXR was solved by difference Fourier refinement from RED. R-free cross validation using 10% of reflections [48] was used throughout all the structure determinations and refinements.

The calculated solvent content of the reduced DsbA crystal form indicated that two DsbA molecules were present in the asymmetric unit. The two highest peaks in the rotation function were at ($\theta_1 = 343.3°$, $\theta_2 = 42.5°$, $\theta_3 = 287.9°$) and ($\theta_1 = 173.0°$, $\theta_2 = 60.0°$, $\theta_3 = 93.0°$) and were 4.1σ and 3.7σ above the mean, respectively. The next highest peak was 3.1σ above the mean. After PC-refinement [46], the two top peaks had the highest correlation coefficients of 0.1183 and 0.1277, respectively. For peak 1, the translation search calculated using X-PLOR gave a maximum at x = 17.47 Å, y = 7.47 Å and z = 27.9 Å with a correlation coefficient of 0.291 (7.0σ above the mean). The translation search with peak 2 from the rotation function gave a maximum at x = 13.44 Å, y = 39.20 Å and z = 12.10 Å, with a correlation coefficient of 0.333 (8.3σ above the mean). The common origin of the second molecule relative to the first was located at (1/2,0,0). When the two molecules were positioned in the asymmetric unit, a correlation coefficient of 0.5704 was obtained. Using all data in the resolution range 10–2.7 Å, the R-factor for this solution was 0.410 and R-free was 0.411.

For OX2, the rotation and translation searches were performed using reflections in the resolution range 15–4 Å. The initial rotation search did not find a clear solution for the single molecule in the asymmetric unit. After PC refinement, however, a peak with a correlation coefficient of 0.331 was obtained at ($\theta_1 = 221.9°$, $\theta_2 = 44.5°$, $\theta_3 = 155.8°$). The next highest peak had a correlation coefficient of < 0.120. The maximum in the translation function was at x = 0.45, z = 0.40 (in fractional coordinates) with a correlation coefficient of 0.607 or 8.1σ above the mean. The initial R-factor and R-free values for reflections in the range 10–3 Å were 0.451 and 0.476, respectively.

Crystallographic refinement

Refinement was performed using X-PLOR v3.1 for OX2 and v3.851 for RED and OXR and was guided by the use of R-free [49]. Rigid body refinement of both RED and OX2 structures was performed by allowing the helical and thioredoxin domains to refine independently. In both cases, this resulted in a significant reduction of R-factor and R-free of 2–4%. Positional and individual B-factor refinement were performed using standard protocols within X-PLOR. For RED (anisotropic overall B-factor correction) and OX2 structures, bulk solvent correction as implemented in X-PLOR was also used. Refinement weights were chosen that strongly restrained the geometric parameters to prevent overfitting of the crystallographic data. Model building was performed using the program O [50]. Waters were included only where spherical density was present above 1.0σ in the $2F_o–F_c$ map and above 3.0σ in the $F_o–F_c$ map, and where the water made stereochemically reasonable hydrogen bonds. Crystallographic and geometric statistics for the final refined models of the DsbA crystal structures are given in Table 2.

For reduced DsbA, residues 29–34 at the active site (including the two cysteines Cys30 and Cys33) of each of the two molecules in the asymmetric unit were excluded from initial crystallographic refinement. After rigid-body refinement, the electron density maps were of sufficient quality to unambiguously model all the active-site residues 29–34, including the reduced conformations of Cys30 and Cys33. The final $2F_o–F_c$ electron density map of the active site of reduced DsbA is shown in Figure 2. The refined model of reduced DsbA and oxidized DsbA in the reduced crystal form excludes mobile residues at the N and C termini (Ala1, Gln2 and Lys189 in both molecules).

In all the protein crystal structures, residues with poorly defined sidechain density were modeled as alanine. For reduced DsbA, these residues are Lys7, Lys14, Lys47, Glu52, Lys55, Lys98, Glu120, Lys132, Asp167 and

Lys183 from both REDA and REDB, plus from REDA only Gln146, Lys158, Ser169, Val173, Gln177 and Tyr184 and from REDB only Glu13, Lys48, Arg103, Ser106, Gln137, Gln164, Gln176 and Ser186.

Similarly, the following residues were modeled as alanine in OXR: for both molecules Lys7, Lys14, Lys47, Lys49, Lys55, Lys87, Lys118, Glu120 and Lys188; plus from OXRA only Asp5, Glu38, Ile42, Lys48, Val54, Lys70, Lys78, Gln137, Arg148, Ser169, Asn170, Met171, Asp172, Val173, Gln177, Tyr184, Ser186 and Gln187; and from OXRB only Gln2, Tyr9, Glu13, Asp67, Gln100, Arg103, Ser106, Asp107, Arg109, Ile117, Glu121, Ser133, Gln146, Lys158 and Gln164.

For OX2, the final model includes all residues except the C-terminal Lys189. The sidechains of residues Glu4, Glu13, Lys48, Lys98, Lys118, Glu120, Lys132, Gln146 and Lys183 were modeled as alanine because of poorly defined sidechain density. Residues Glu85, Ser106, Ser133 and Ser186 were modeled with two conformations, each of half occupancy.

Structure validation and analysis

The final structures were validated using the program PROCHECK [51]. The structures were superimposed and rmsd calculations were performed using the program O [50]. An analysis of the hinge angle between the two domains of DsbA was performed using the program HINGEFIND [22].

Accession numbers

Coordinates of OX2, OXR and RED have been deposited at the PDB [26] with accession codes 1A2J, 1A2M and 1A2L, respectively. Structure factors have also been deposited. Coordinates of the 1.7 Å refined crystal structure of oxidized DsbA in the *C*2 crystal form (OX1) used in this analysis are available from the PDB with accession code 1FVK.

Acknowledgements

We gratefully acknowledge Judy Halliday for help with protein expression, Alun Jones for help with mass spectrometric data measurement and analysis and Willy Wriggers for help with using HINGEFIND. We also thank Rudi Glockshuber, Martina Huber-Wunderlich and Horst Schirra for critical comments and we are grateful to Margarita Ingelman and Hans Eklund for providing coordinates of reduced T4 glutaredoxin. This work is supported by a grant from the Australian Research Council (A09531886), a Queen Elizabeth II Fellowship to J.L.M. and an NIH grant to J.C.A.B.

References

1. Martin, J.L. (1995). Thioredoxin - a fold for all reasons. *Structure,* **3**, 245-250.
2. Missiakas, D., Georgopoulos, C. & Raina, S. (1994). The *Escherichia coli dsbC* (*xprA*) gene encodes a periplasmic protein involved in disulfide bond formation. *EMBO J.* **13**, 2013-2020.
3. Missiakas, D., Schwager, F. & Raina, S. (1995). Identification and characterization of a new disulfide isomerase-like protein (DsbD) in *Escherichia coli*. *EMBO J.* **14**, 3415-3424.
4. Fabianek, R.A., *et al.*, & Thöny-Meyer, L. (1997). Characterization of the *Bradyrhizobium japonicum* CycY protein, a membrane-anchored periplasmic thioredoxin that may play a role as a reductant in the biogenesis of *c*-type cytochromes. *J. Biol. Chem.* **272**, 4467-4473.
5. Loferer, H., Bott, M. & Hennecke, H. (1993). *Bradyrhizobium japonicum* TlpA, a novel membrane-anchored thioredoxin-like protein involved in the biogenesis of cytochrome aa^3 and development of symbiosis. *EMBO J.* **12**, 3373-3383.
6. Martin, J.L., Bardwell, J.C.A. & Kuriyan, J. (1993). Crystal structure of the DsbA protein required for disulphide bond formation *in vivo*. *Nature* **365**, 464-468.
7. Kemmink, J., Darby, N.J., Dijkstra, K., Nilges, M. & Creighton, T.E. (1996). Structure determination of the N-terminal thioredoxin-like domain of protein disulfide isomerase using multidimensional heteronuclear 13C/15N NMR spectroscopy. *Biochemistry* **35**, 7684-7691.
8. Holmgren, A. (1985). Thioredoxin. *Annu. Rev. Biochem.* **54**, 237-271.
9. Darby, N.J., Freedman, R.B. & Creighton, T.E. (1994). Dissecting the mechanism of protein disulfide isomerase - catalysis of disulfide bond formation in a model peptide. *Biochemistry* **33**, 7937-7947.
10. Kemmink, J., Darby, N.J., Dijkstra, K., Nilges, M. & Creighton, T.E. (1997). The folding catalyst protein disulfide isomerase is constructed of active and inactive thioredoxin modules. *Curr. Biol.* **7**, 239-245.
11. Wunderlich, M. & Glockshuber, R. (1993). Redox properties of protein disulfide isomerase (DsbA) from *Escherichia coli*. *Protein Sci.* **2**, 717-726.
12. Zapun, A., Bardwell, J.C.A. & Creighton, T.E. (1993). The reactive and destabilising disulfide bond of DsbA, a protein required for protein disulfide bond formation *in vivo*. *Biochemistry* **32**, 5083-5092.
13. Lundström, J. & Holmgren, A. (1993). Determination of the reduction-oxidation potential of the thioredoxin-like domains of protein disulfide isomerase from the equilibrium with glutathione and thioredoxin. *Biochemistry* **32**, 6649-6655.
14. Darby, N.J. & Creighton, T.E. (1995). Characterization of the active site cysteine residues of the thioredoxin-like domains of protein disulfide isomerase. *Biochemistry* **34**, 16770-16780.
15. Lin, T.-Y. & Kim, P.S. (1989). Urea dependence of thiol-disulfide equilibria in thioredoxin: confirmation of the linkage relationship and a sensitive assay for structure. *Biochemistry* **28**, 5282-5287.
16. Wunderlich, M., Jaenicke, R. & Glockshuber, R. (1993). The redox properties of protein disulfide isomerase (DsbA) of *Escherichia coli* result from a tense conformation of its oxidized form. *J. Mol. Biol.* **233**, 559-566.
17. Nelson, J.W. & Creighton, T.E. (1994). Reactivity and ionization of the active site cysteine residues of DsbA, a protein required for disulfide bond formation in vivo. *Biochemistry* **33**, 5974-5983.
18. Grauschopf, U., *et al.*, & Bardwell, J.C.A. (1995). Why is DsbA such an oxidizing disulfide catalyst? *Cell* **83**, 947-955.
19. Kortemme, T., Darby, N.J. & Creighton, T.E. (1996). Electrostatic interactions in the active site of the N-terminal thioredoxin-like domain of protein disulfide isomerase. *Biochemistry* **35**, 14503-14511.
20. Guddat, L.W., Bardwell, J.C.A., Zander, T. & Martin, J.L. (1997). The uncharged surface features surrounding the active-site of *E. coli* DsbA are conserved and are implicated in peptide binding. *Protein Sci.* **6**, 1148-1156.
21. Guddat, L.W., *et al.*, & Martin, J.L. (1997). Structural analysis of three His32 mutants of DsbA: support for an electrostatic role of His32 in DsbA stability. *Protein Sci.* **6**, 1893-1900.
22. Wriggers, W. & Schulten, K. (1997). Protein domain movements: detection of rigid domains and visualization of hinges in comparisons of atomic coordinates. *Proteins* **29**, 1-14.
23. Jeng, M.-F., *et al.*, & Dyson, H.J. (1994). High-resolution solution structures of oxidized and reduced *Escherichia coli* thioredoxin. *Structure* **2**, 853-868.
24. Qin, J., Clore, G.M. & Gronenborn, A.M. (1994). The high-resolution three-dimensional solution structures of the oxidized and reduced states of human thioredoxin. *Structure* **2**, 503-522.
25. Weichsel, A., Gasdaska, J.R., Powis, G. & Montfort, W.R. (1996). Crystal structure of reduced, oxidized, and mutated human thioredoxins: evidence for a regulatory homodimer. *Structure* **4**, 735-751.
26. Bernstein, F.C., *et al.*, & Tasumi, M. (1977). The protein data bank: a computer-based archival file for macromolecular structures. *J. Mol. Biol.* **112**, 535-542.
27. Ingelman, M., Nordlund, P. & Eklund, H. (1995). The structure of a reduced mutant T4 glutaredoxin. *FEBS Lett.* **370**, 209-211.
28. Missiakas, D., Georgopoulos, C. & Raina, S. (1993). Identification and characterization of the *Escherichia coli* gene *dsbB*, whose product is involved in the formation of disulfide bonds *in vivo*. *Proc. Natl Acad. Sci. USA* **90**, 7084-7088.
29. Kerr, K.A., Ashmore, J.P. & Koetzle, T.F. (1975). A neutron diffraction study of L-cysteine. *Acta Crystallogr.* **B31**, 2022 - 2026.
30. Adman, E., Watenpaugh, K.D. & Jensen, L.H. (1975). NH...S hydrogen bonds in *Peptococcus aerogenes* ferredoxin, *Clostridium pasteurianum* rubredoxin, and *Chromatium* high potential iron protein. *Proc. Natl Acad. Sci. USA* **72**, 4854-4858.
31. Gregoret, L.M., Rader, S.D., Fletterick, R.J. & Cohen, F.E. (1991). Hydrogen bonds involving sulfur atoms in proteins. *Proteins* **9**, 99-107.
32. Andrews, P.R., Craik, D.J. & Martin, J.L. (1984). Functional group contributions to drug-receptor interactions. *J. Med. Chem.* **27**, 1648-1657.
33. Fersht, A.R., *et al.*, & Winter, G. (1987). Hydrogen bonding and biological specificity analysed by protein engineering. *Nature* **314**, 235-238.
34. Hol, W.G. (1985). The role of the α-helix dipole in protein function and structure. *Prog. Biophys. Mol. Biol.* **45**, 149-195.

35. Kortemme, T. & Creighton, T.E. (1995). Ionisation of cysteine residues at the termini of model α-helical peptides. Relevance to unusual thiol pK_a values in proteins of the thioredoxin family. *J. Mol. Biol.* **253**, 799-812.
36. Kallis, G.-B. & Holmgren, A. (1980). Differential reactivity of the functional sulfhydryl groups of cysteine-32 and cysteine-35 present in the reduced form of thioredoxin from *Escherichia coli*. *J. Biol. Chem.* **255**, 10261-10265.
37. Dyson, H.J., Tennant, L.L. & Holmgren, A. (1991). Proton-transfer effects in the active-site region of *Escherichia coli* thioredoxin using two-dimensional 1H NMR. *Biochemistry* **30**, 4262-4268.
38. Forman-Kay, J.D., Clore, G.M. & Gronenborn, A.M. (1992). Relationship between electrostatics and redox function in human thioredoxin: characterization of pH titration shifts using two-dimensional homo- and heteronuclear NMR. *Biochemistry* **31**, 3442-3452.
39. Gan, Z.-R., Sardana, M.K., Jacobs, J.W. & Polokoff, M.A. (1990). Yeast thioltransferase - the active site cysteines display differential reactivity. *Arch. Biochem. Biophys.* **282**, 110-115.
40. Mieyal, J.J., Starke, D.W., Gravina, S.A. & Hocevar, B.A. (1991). Thioltransferase in human red blood cells: kinetics and equilibrium. *Biochemistry* **30**, 8883-8891.
41. Yang, Y. & Wells, W.W. (1991). Identification and characterization of the functional amino acids at the active center of pig liver thioltransferase by site-directed mutagenesis. *J. Biol. Chem.* **266**, 12759-12765.
42. Schirra, H.J., *et al.,* & Glockshuber, R. (1998). Structure of reduced DsbA from Escherichia coli in solution. *Biochemistry* **37**, 6263-6276.
43. Bardwell, J.C.A., McGovern, K. & Beckwith, J. (1991). Identification of a protein required for disulfide bond formation *in vivo*. *Cell* **67**, 581-589.
44. Martin, J.L., Waksman, G., Bardwell, J.C.A., Beckwith, J. & Kuriyan, J. (1993). Crystallization of DsbA, an *Escherichia coli* protein required for disulphide bond formation *in vivo*. *J. Mol. Biol.* **230**, 1097-1100.
45. Otwinowski, Z. & Minor, W. (1996). Processing of X-ray diffraction data collected in oscillation mode. *Methods Enzymol.* **276**, 307-326.
46. Brünger, A.T. (1990). Extension of molecular replacement: a new search strategy based on Patterson correlation refinement. *Acta Crystallogr.* **A46**, 46-57.
47. Brünger, A.T. (1992). *X-PLOR (Version 3.1) Manual*. Yale University, New Haven, CT, USA.
48. Brünger, A.T. (1992). Free R value: a novel statistical quantity for assessing the accuracy of crystal structures. *Nature* **355**, 472-475.
49. Kleywegt, G.J. & Brünger, A.T. (1996). Checking your imagination: applications of the free R value. *Structure* **4**, 897-904.
50. Jones, T.A., Zou, J.Y., Cowan, S.W. & Kjeldgaard, M. (1991). Improved methods for building protein models in electron density maps and the location of errors in these models. *Acta Crystallogr.* **A47**, 110-119.
51. Laskowski, R.A., MacArthur, M.W., Moss, D.S. & Thornton, J.M. (1993). PROCHECK: a program to check the stereochemical quality of protein structures. *J. Appl. Crystallogr.* **26**, 283-291.
52. Kraulis, P.J. (1991). MOLSCRIPT: a program to produce both detailed and schematic plots of protein structures. *J. Appl. Crystallogr.* **24**, 946-950.
53. Bacon, D.J. & Anderson, W.F. (1988). A fast algorithm for rendering space filling molecular pictures. *J. Mol. Graphics* **6**, 219-222.
54. Merritt, E.A. & Murphy, M.E.P. (1994). Raster3D version 2.0. A program for photorealistic molecular graphics. *Acta Crystallogr.* **D50**, 869-873.
55. Evans, S.V. (1993). SETOR: hardware-lighted three-dimensional solid model representations of macromolecules. *J. Mol. Graphics* **11**, 134-138.